

# An Analysis of the Pressure Build-Up Inside a Reacting Pellet During Gas Solid Reactions

T. DEB ROY AND K. P. ABRAHAM

A method has been outlined for the calculation of the pressure gradient that can exist within the reacted shell when a spherical pellet reacts with a gas and undergoes a transport controlled topochemical reaction. It is known that pressure gradients can arise because of Knudsen flow existing in the reacted shell with small pores and the reactant gas having a different diffusivity than that of the product gas. The phenomena can be represented by a boundary value problem involving a set of partial differential equations with a moving boundary, incorporating time and positional dependence of diffusivities of the reactant and product gases. In the present work, the resulting equations have been solved numerically. A study has been made of the influence of the relevant parameters like total and Knudsen diffusivity ratios of the reactant and product gases, the porosity to tortuosity ratio of the reacted shell, the Biot modulus, the equilibrium constant of the reaction and the viscous flow parameter on the pressure build up inside the reacted shell.

SEVERAL kinetic investigations on gas solid reactions have been carried out in the recent past and in the majority of cases, experiments were performed with the pellets of the reacting solid suspended in a flowing stream of the reacting gas. Attempts were then made to interpret results with the help of mathematical models. In many kinetic experiments using dense pellets, it has been found that the reaction could be described in terms of a topochemical model as shown in Fig. 1. Here the reaction front is constantly receding towards the center of the pellet as the reaction proceeds. In many cases the reaction is transport controlled and the reaction rate is strongly dependent on the rate of diffusion of the gaseous species through a porous product layer to a reacting interface which separates the reactant solid from the converted solid product. The gaseous diffusion and flow involved in such a problem is dependent on the nature of the solid product, properties of the gaseous species involved and the experimental conditions. Depending on these factors the diffusion involved may be molecular, Knudsen or a mixed diffusion. In those cases where the pore size is small and Knudsen diffusion is important, the effective diffusivities of the reactant and product gases are not identical. Lu and Bitsianes<sup>1</sup> have pointed out that in such cases, a pressure gradient can exist in the case of a gas solid reaction system whose rate is controlled by gaseous transport to the reaction front. For example it is known from previous experiments that Knudsen diffusion is prominent in the transport of gases through the product layer, in the case of reduction of  $\text{Fe}_2\text{O}_3$  by  $\text{H}_2$  and reduction of  $\text{NiO}$  by  $\text{CO}$ <sup>3</sup> and  $\text{H}_2$ <sup>4</sup>. In these cases a pressure build up can occur within the reacted shell. The nonhomogeneity of pressure inside a reacting solid is quite possible and this must be taken into account for a meaningful interpretation of experimental results.

In this paper an attempt has been made for a quan-

titative theoretical analysis of the problem under discussion. The treatment is given for radial diffusion phenomena involving spheres. The results of the diffusion studies of Mason and co-workers<sup>5,6</sup> have been employed for the formulation of the problem. It has been shown that the phenomena could be described in terms of a boundary value problem involving a set of nonlinear partial differential equations with a moving boundary. Pressure dependence of diffusivity has been incorporated in the analysis. The resulting equations were solved numerically. A study has been made of the effect of varying the dimensionless parameters involving diffusivity, molecular weight of the reacting and product gases, Biot modulus, porosity-tortuosity ratio, equilibrium constant and the viscous flow parameter on the pressure build up.

## FORMULATION

Consider a noncatalytic reaction of the following type taking place between solid I and gas 1 to form products, solid II and gas 2,

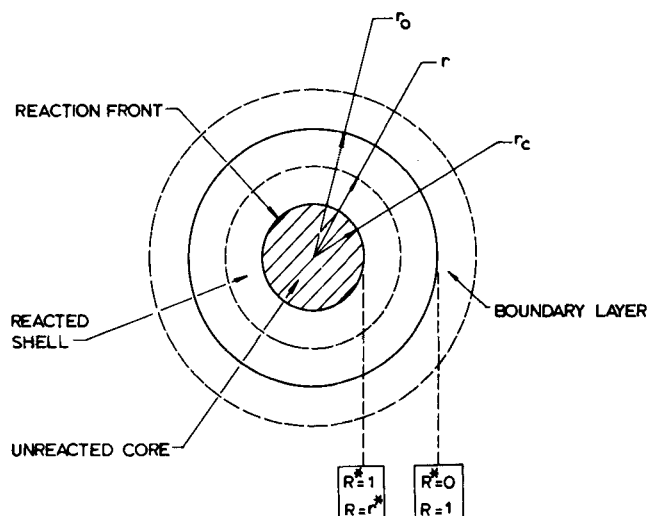


Fig. 1—Topochemical reaction model.

T. DEB ROY and K. P. ABRAHAM are Research Student and Professor, respectively, Department of Metallurgy, Indian Institute of Science, Bangalore-560012, India.

Manuscript submitted March 7, 1973.

$$\text{Solid I} + \text{Gas 1} = \text{Solid II} + \text{Gas 2} \quad [1]$$

The following assumptions are made in the present treatment.

1) The reaction is topochemical and takes place under isothermal conditions.

2) The reaction is considered to be equimolar with generation of one mole of product gas for each mole of reactant gas consumed.

3) The flow rate of the reactant gas is high enough so that there is no gas starvation and the reactant gas concentration in the bulk phase can be approximated to the total gas concentration in the bulk phase.

4) The viscosity of the gas phase is independent of the composition and pressure. This assumption simplifies computation problem greatly and is considered worthwhile in view of the small error in flux due to this assumption under the conditions commonly encountered in gas solid reactions.

5) Structural changes like swelling or sintering of the pellet have been neglected and the gases are considered to behave ideally.

Mason and co-workers<sup>6</sup> have developed a set of expressions for the flux of individual gaseous components 1 and 2 in a binary gas mixture. Their expressions for the flux of individual gaseous components inside a porous solid is given by the following equations.

$$J_1 = -(D_1)^{\text{eff}} \frac{\partial C_1}{\partial r} + x_1 \delta_1 J - x_1(1 - \delta_1) \frac{B_0 F_c P}{\eta R_G T_K} \frac{dP}{dr} \quad [2]$$

$$J - \beta_1 J_1 = \frac{-(D_2^K)^{\text{eff}}}{R_G T_K} \left[ 1 + \frac{B_0 F_c P}{\eta (\bar{D}_K)^{\text{eff}}} \right] \frac{dP}{dr} \quad [3]$$

where

$$\delta_1 = \frac{D_1}{D_G};$$

$$\frac{1}{(\bar{D}_K)^{\text{eff}}} = \frac{T}{\epsilon} \left[ \frac{x_1}{D_1^K} + \frac{x_2}{D_2^K} \right]$$

and

$$B_0 = \frac{r_p^2 \epsilon}{8T}$$

In the above equations, the factor  $F_c$  represents a conversion factor for the dimensional consistency.  $B_0$  is a constant characteristic of the solid alone. For a cylindrical capillary the value of  $B_0$  is  $r_p^2/8$ . The factor  $\epsilon/T$  is introduced to take into account the porosity of the product solid through which the gas flow takes place, and the inevitable deviation of the pores from idealized cylindrical geometry. Radially outward flow is taken as positive in these two expressions and this convention will be maintained throughout.

Evans<sup>7</sup> has shown that an error will be introduced in the magnitude of the flux  $J_1$  by neglecting the viscous flow terms in the flux equations. According to him, this error is only about 10 pct for conditions typical of gas solid reactions and may be negligible when the pore size of the solid is very small. However, while considering a general case for the pressure build up, it will be desirable to take into account all the three terms including the viscous flow term in the flux Eq. [2]. Eqs. [2] and [3] could be rearranged to get the following two expressions.

$$J_1^* = -F_1 \frac{\partial C_1^*}{\partial R} + F_2 x_1 J^* - (1 - F_2) B_0^* C_1^* \frac{\partial P^*}{\partial R} \quad [4]$$

$$J^* - \beta_1 J_1^* = K_1 \frac{\partial P^*}{\partial R} - (1 - x_1 \beta_1) B_0^* P^* \frac{\partial P^*}{\partial R} \quad [5]$$

where

$$F_1 = \frac{D_1}{D_G} = \frac{(D_1)^{\text{eff}}}{(D_G^0)^{\text{eff}}}$$

$$F_2 = \frac{D_1}{D_G} = \frac{(D_1)^{\text{eff}}}{(D_G)^{\text{eff}}}$$

and

$$K_1 = \frac{D_2^K}{D_G^0} = \frac{(D_2^K)^{\text{eff}}}{(D_G^0)^{\text{eff}}}$$

Also the rate of accumulation of component 1 is given by the following equation.

$$-\epsilon \frac{\partial C_1^*}{\partial \tau} = \frac{1}{R^2} \frac{\partial}{\partial R} (R^2 J_1^*) \quad [6]$$

Similarly the over-all accumulation rate is expressed by Eq. [7].

$$-\epsilon \frac{\partial P^*}{\partial \tau} = \frac{1}{R^2} \frac{\partial}{\partial R} (R^2 J^*) \quad [7]$$

$F_1$  and  $F_2$  in Eq. [4] can be expressed in terms of the ratio of the effective diffusivities and the ratio of the square roots of the molecular weights of component 1 and 2 respectively by the following two equations.

$$F_1 = \frac{\beta - \Delta}{P^*(\beta - 1)} \quad [8]$$

$$F_2 = P^* \cdot F_1 \quad [9]$$

Also

$$K_1 = \frac{\beta - \Delta^0}{\beta (\Delta^0 - 1)} \quad [10]$$

While  $\beta$  is independent of pressure,  $\Delta$  implicitly contains gaseous molecular diffusivity which is inversely proportional to pressure. Thus  $F_1$  and  $F_2$  are functions of  $R$  and  $\tau$ . The variation of  $\Delta$  resulting from pressure variation can be expressed by the following relationship.

$$\Delta = \frac{P^*(\beta - \Delta^0) + \beta (\Delta^0 - 1)}{P^*(\beta - \Delta^0) + (\Delta^0 - 1)} \quad [11]$$

From the definition of flux through the boundary layer, the following relationship can be written.

$$J_1^* |_{R=1} = \left[ \frac{1}{\frac{\epsilon}{T} B_i^M} (C_1^* - 1) + C_1^* J^* \right]_{R=1} \quad [12]$$

Since the pellet surface is exposed to atmosphere, the value of total pressure at the pellet surface is the same as that in the bulk.

Therefore

$$P^* |_{R=1} = 1 \quad [13]$$

Also as the reaction is considered to be a transport controlled one, chemical equilibrium is assumed to prevail at the reaction front.

$$\frac{P^*}{C_1^*} \Big|_{R=r^*} = 1 + K_{\text{eq}} \quad [14]$$

The unreacted core is considered impervious to gases in consistency with the topochemical reaction model and since the reaction is equimolar, the following relationship is valid.

$$J^*|_{R=r^*} = 0 \quad [15]$$

Also since the reaction is controlled by the transport of the reacting species to the reaction interface, the following condition for the movement of the boundary can be written down.

$$J_1^*|_{R=r^*} = -\rho^* \frac{dr^*}{d\tau} \quad [16]$$

Thus Eqs. [4] to [16] describe the phenomena under discussion. Since these equations could not be solved analytically, numerical techniques have been employed for the solution. A brief account of the technique used is given in the appendix.

### RESULTS

The results are shown in graphical form in Figs. 2 to 6. In Figs. 2 to 5 the dimensionless pressure at the reaction front is plotted against fraction converted  $F$  ( $= 1 - r^{*3}$ ). The values of the parameters used which affect the pressure build up are those typical of gas solid reactions reported in literature. In these graphs the value of  $B_0^*$  is taken to be zero, because in the majority of cases where the pore radius is small and Knudsen diffusion is important, the viscous flow parameter (and the value of  $B_0^*$ ) is negligibly small. However to show the effect of  $B_0^*$  on the pressure build up, the effect of varying  $B_0^*$  from 0 to 0.5 on the pressure build up is shown in Fig. 6. Also the profiles of dimensionless pressure and diffusivity ratio  $\Delta$  inside the reacted shell are plotted corresponding to different  $r^*$  values. The values of different parameters used for these computations are given in the figure captions.

### DISCUSSION

An examination of Eqs. [4] to [16] shows that the factors which contribute towards the pressure build up

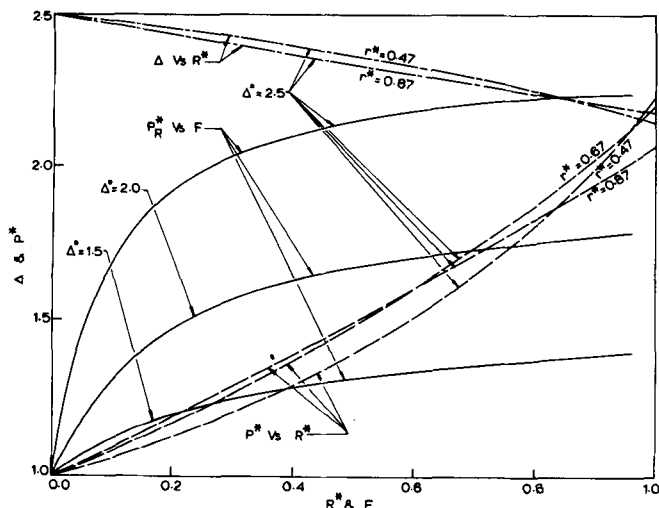


Fig. 2—Effect of variation of the diffusivity ratio  $\Delta^0$  on the pressure build up,  $\beta = 3.0$ ,  $B_0^* (\epsilon/T) = 0.15$ ,  $K_{eq} = 1000$ ,  $\rho^* = 4774$  and  $\epsilon = 0.50$ .

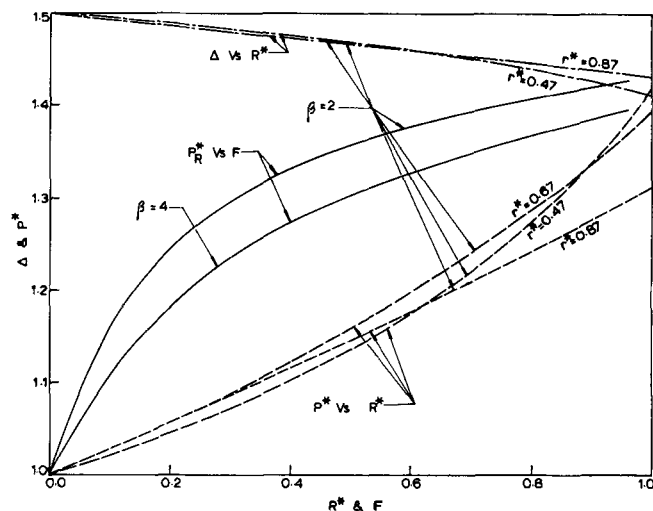


Fig. 3—Effect of variation of the diffusivity ratio  $\beta$  on the pressure build up,  $\Delta^0 = 1.5$ ,  $B_0^* (\epsilon/T) = 0.15$ ,  $K_{eq} = 1000$ ,  $\rho^* = 4774$  and  $\epsilon = 0.50$ .

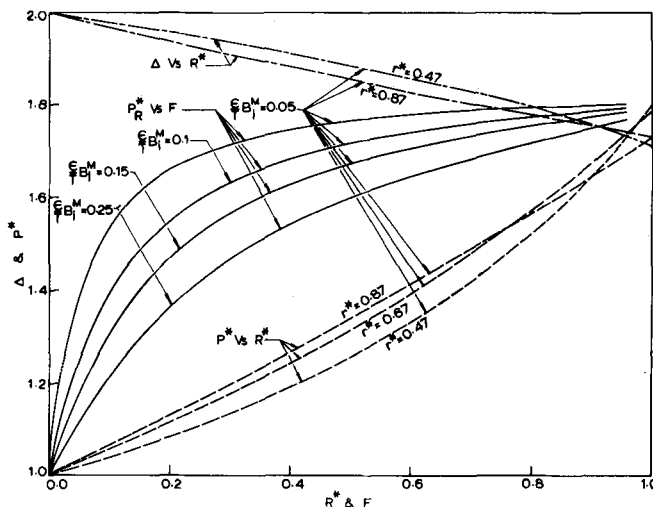


Fig. 4—Effect of variation of  $B_0^* (\epsilon/T)$  on the pressure build up,  $\Delta^0 = 2.0$ ,  $\beta = 3.0$ ,  $K_{eq} = 1000$ ,  $\rho^* = 4774$ ,  $\epsilon = 0.50$ .

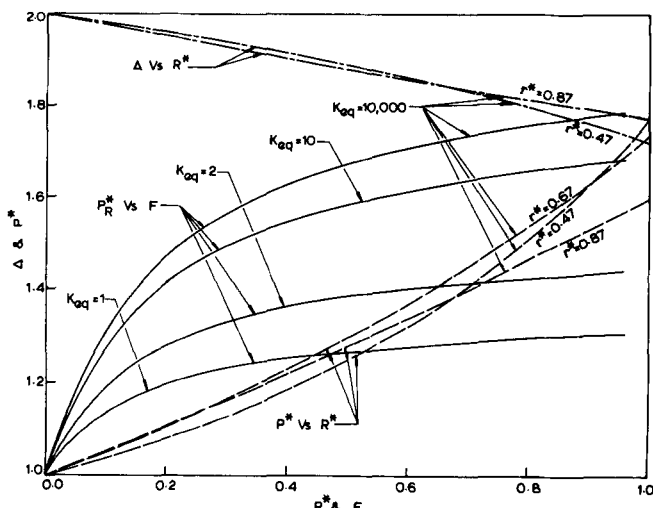


Fig. 5—Effect of variation of equilibrium constant on the pressure build up,  $\Delta^0 = 2.0$ ,  $\beta = 3.0$ ,  $B_0^* (\epsilon/T) = 0.15$ ,  $\rho^* = 4774$ ,  $\epsilon = 0.50$ .

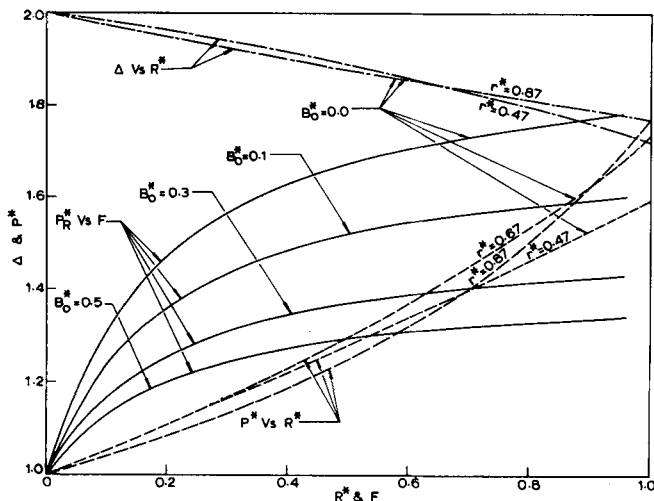


Fig. 6—Effect of variation of dimensionless viscous flow parameter  $B_0^*$  on the pressure build up,  $\Delta^0 = 2.0$ ,  $\beta = 3.0$ ,  $B_i^M(\epsilon/T) = 0.15$ ,  $K_{eq} = 1000$ ,  $\rho^* = 4774$ ,  $\epsilon = 0.50$ .

during the reaction are the diffusivity ratios  $\Delta^0$  and  $\beta$ , the equilibrium constant  $K_{eq}$ , the dimensionless viscous flow parameter  $B_0^*$ , the product  $B_i^M(\epsilon/T)$ , the dimensionless density  $\rho^*$ , and porosity  $\epsilon$ .

Of these parameters, the porosity term  $\epsilon$  appears in Eqs. [6] and [7] (as distinctly from  $B_i^M(\epsilon/T)$ ) as a multiplying factor of  $\partial P^*/\partial \tau$  and  $\partial C_1^*/\partial \tau$ . Even though  $\partial P^*/\partial \tau$  and  $\partial C_1^*/\partial \tau$  are not taken as zero in the present work, the magnitudes of these derivatives are small. In view of the fact that an analytical solution of the present problem could not be developed, an examination of the effect of  $\epsilon$  (as distinctly from  $B_i^M(\epsilon/T)$ ) on the pressure build up is not attempted to avoid any possible uncertainty due to computation. However, since  $\partial C_1^*/\partial \tau$  and  $\partial P^*/\partial \tau$  are small, it is considered logical to examine the effect of  $\epsilon$  from a study of the variable  $B_i^M(\epsilon/T)$ .

Also the variable  $\rho^*$  appears only in the condition for the movement of the interface according to Eq. [16]. Thus a change in  $\rho^*$  induces a change in the rate of movement of the interface and in Figs. 2 to 6, the effect of changing  $\rho^*$  would be virtually, equivalent to a compression or elongation of the "F" axis, and consequently the effect of  $\rho^*$  on the pressure build up is not analyzed separately.

It is evident that in the case of an irreversible reaction the pressure build up is likely to be more with increase in the ratio of the diffusivities  $D_1^0/D_2^0 (= \Delta^0)$ , because of the accumulation of the product gas. This trend is easily seen in Fig. 2.

The effect of varying  $\beta$  on the pressure build up can be examined by considering Eqs. [17] and [18] derived from the definitions of  $\beta$  and  $\Delta^0$ .

$$\frac{D_1^K}{D_G^0} = \frac{\beta - \Delta^0}{\Delta^0 - 1} \quad [17]$$

$$\frac{D_2^K}{D_G^0} = \frac{1 - \Delta^0/\beta}{\Delta^0 - 1} \quad [18]$$

It is observed from the above equations that an increase in  $\beta$  keeping  $\Delta^0$  constant leads to an increase in the ratios  $D_1^K/D_G^0$  and  $D_2^K/D_G^0$ . This in other words means that the molecular diffusion rather than Knud-

sen diffusion has a larger share in determining the diffusivities of components 1 and 2 through the reacted shell. The larger the contribution due to molecular diffusion, the smaller will be the pressure build up and hence the pressure build up takes place at a comparatively slower rate under the conditions discussed. This trend is shown in Fig. 3.

Fig. 4 shows the effect of varying the product of Blot modulus and the porosity to tortuosity ratio of the product layer. A higher value of  $\epsilon/T$ , considering  $B_i^M$  constant, means that less "resistance" is offered to the reaction by the step involving shell layer diffusion. Thus a lag in the build up of pressure is exhibited on increasing  $B_i^M(\epsilon/T)$ . Similarly an increase in  $B_i^M$  keeping  $\epsilon/T$  as constant is equivalent to a higher contribution of the external transport resistance towards the total resistance of the reaction, and a delay is observed in the accumulation of pressure. This behavior can be seen in Fig. 4.

Fig. 5 shows the variation of the pressure accumulation with the equilibrium constant of the reaction. Since the reaction is analyzed as a transport controlled one, a decrease in  $K_{eq}$  from a very high to a low value would cause a comparatively smaller concentration of the reactant gas at the reaction front. It can be seen that a substantial decrease in  $K_{eq}$  would increase the ratio  $(C_2^R - C_2^b)/(C_1^b - C_1^R)$ , consequently the ratio of the rate of outflow to the inflow of the gases increases, resulting in the lower pressure build up.

In Fig. 6 the effect of the variation of the dimensionless viscous flow parameter on the pressure build up is shown. Since the viscous flow parameter is proportional to the square of the pore radius,  $B_0^*$  is normally small in those cases where Knudsen diffusion is important. It is seen from Fig. 6 that the smaller the viscous flow parameter, the larger is the pressure build up. This is physically justified since the smaller the pore radius the larger is the contribution of the Knudsen diffusion.

The pressure distributions inside the reacted shell for different values of  $r^*$  are plotted in Figs. 2 to 6. It is observed that for a large value of  $r^*$  corresponding to about 30 pct conversion, the pressure distribution is found to be approximately linear, which is also to be expected in the thin shells under consideration. The variation of  $\Delta$  resulting from the time and positional dependence of pressure is also shown in these figures.

It is obvious that the present analysis is relevant to systems giving rise to a product layer which is sufficiently strong and tough to withstand the development of the higher pressure.

## SUMMARY

1) Appreciable pressure gradient can exist within the reacted solid during a transport controlled topochemical reaction in all the cases where the pore size is sufficiently small for Knudsen diffusion to be important and the reactant gas has a diffusivity different from that of the product gas.

2) For a transport controlled topochemical reaction, the dimensionless pressure build up depends on the ratios of the diffusivities  $\Delta^0$  and  $\beta$ , the product of

porosity-tortuosity ratio  $\epsilon/T$  and the Biot modulus  $B_i^M$ , the equilibrium constant  $K_{eq}$  and the dimensionless viscous flow parameter  $B_0^*$ .

3) A method has been outlined for the quantitative calculation of the pressure gradient inside the reacted shell.

4) The effect of the relevant variables on the pressure build up is analyzed and the results are given in graphical form.

5) The pressure profiles inside the reacted shell are approximately linear in the initial stages till about 30 pct of the reaction is over.

#### ACKNOWLEDGMENTS

The authors are thankful to Dr. A. K. Lahiri for helpful discussions.

#### NOMENCLATURE

$B_0$	Viscous flow parameter, sq cm
$C$	Total concentration of the gas, g-mole per cu cm
$C_1$	Concentration of component 1, g-mole per cu cm
$D_G$	Binary molecular diffusivity, sq cm
$D_i^K$	Knudsen diffusivity of component $i$ $\left[ = \frac{2}{3} r_p \left( \frac{8R_k T K}{M_i \pi} \right)^{1/2} \right]$ , sq cm
$D_i$	Total diffusion coefficient of component $i$ , $\left[ = \left( \frac{1}{D_G} + \frac{1}{D_i^K} \right)^{-1} \right]$ , sq cm
$(D_i)^{eff}$	Effective total diffusion coefficient of component $i$ , $\left[ = D_i \frac{\epsilon}{T} \right]$ , sq cm
$(D_i^K)^{eff}$	Effective Knudsen diffusion coefficient of component $i$ , $\left[ = D_i^K \frac{\epsilon}{T} \right]$ , sq cm
$(D_G)^{eff}$	Effective binary molecular diffusivity, $\left[ = D_G \frac{\epsilon}{T} \right]$ , sq cm
$F_c$	Conversion factor, $10^6$ g per atm cm sq s
$J$	Flux, g-mole per sq cm s
$P$	Pressure at any point inside the pellet, atm.
$P_0$	Atmospheric pressure, atm.
$R_G$	Gas constant, cu cm atm per g-mole K
$R_K$	Gas constant, g sq cm per sq sec g-mole K
$M_i$	Molecular weight of species $i$ , g per g-mole
$r$	Distance from the center of the reacting pellet, cm
$r_0$	Original radius of the pellet, cm
$r_c$	Radius of the reaction front, cm
$r_p$	Average radius of the pores, cm
$t$	Time, s
$\alpha$	Mass transfer coefficient, cm per s
$\eta$	Viscosity of the gas phase, g per s cm
$\rho_0$	Molar density of the reacting solid, g-mole per cu cm

#### Dimensionless Variables

$B_i^M$	Biot modulus, $\frac{D_G}{\alpha r_0}$
$c_1^*$	Dimensionless concentration of component 1, $c_1/c^b$
$B_0^*$	Dimensionless viscous flow parameter, $\frac{B_0 P_0 F_c}{(D_G^0)^{eff}}$
$F$	Fractional conversion, $1 - r^{*3}$
$J^*$	Flux, $\frac{J r_0}{(D_G^0)^{eff} C^b}$
$P^*$	Dimensionless pressure, $P/P^b$
$R$	Dimensionless radius in the reacted shell, $\frac{r}{r_0}$ , $r_c \leq r \leq r_0$
$R^*$	Dimensionless distance, $\frac{1-R}{1-r^*}$
$r^*$	Dimensionless radius of the reaction front, $r_c/r_0$
$T$	Tortuosity factor in the porous solid
$K_{eq}$	Equilibrium constant for reaction [1]
$x$	Fraction of a particular gaseous component
$\beta$	Dimensionless molecular weight, $\left[ \frac{M_2}{M_1} \right]^{1/2} = \frac{D_1^K}{D_2^K}$
$\Delta$	Dimensionless diffusivity $D_1/D_2$
$\beta_1$	$1 - 1/\beta$
$\delta_1$	$D_1/D_G$
$\rho^*$	Dimensionless density, $\rho_0/C^b$
$\epsilon$	Porosity of the product solid
$\tau$	Dimensionless time, $\frac{t (D_G^0)^{eff}}{r_0^2}$

#### Subscripts

1	Value for component 1
2	Value for component 2
$G$	Value for gas
$k$	Value for Knudsen diffusion
$R$	Value for reaction front
av	Average value

#### Superscripts

$b$	Value for the bulk phase
eff	Effective value
0	Value at one atmosphere pressure.

#### APPENDIX

##### Numerical Scheme for the Solution of the Differential Equations

An implicit difference scheme has been employed for the solution of the equations. In order to restrict the total integration steps to a finite predictable value, varied time increments similar to that used by Douglas *et al.*<sup>8</sup> have been used. In order to keep the moving boundary at the rightmost mesh point at all time levels of computation, the following substitution is made in Eqs. [4] to [7].

$$R^* = \frac{1-R}{1-r^*} \quad [19]$$

A similar transformation was used by Lotkin<sup>9</sup> in the calculation of heat flow in melting solids.

Since the required solution is the evaluation of  $P^*$  and  $C_1^*$  for all predetermined values of  $R$  and also at all levels of computation time  $\tau$ , Eqs. [4] to [7] have been rearranged to eliminate  $J^*$  and  $J_1^*$  after a substitution given by Eq. [19] is made. The resulting equations have been expressed by implicit central difference scheme for the interior grid points and backward difference scheme for the two boundaries. For evaluation of  $\partial C_1^*/\partial \tau$  the following substitutional concentration time derivative similar to the one used by Murray and Landis<sup>10</sup> was used to take into account the movement of the interface.

$$\frac{\partial C_1^*}{\partial \tau} = \frac{dC_1^*}{d\tau} - \frac{\partial C_1^*}{\partial R^*} \frac{dR^*}{d\tau} \quad [20]$$

$dR^*/d\tau$  signifies changes in the grid dimension resulting from the movement of the interface with time. A similar expression was used for the evaluation of  $\partial P^*/\partial \tau$ . The time increment necessary for the predetermined movement of the grid was found using Eq. [16].

Computations revealed that a value of  $\Delta r^* = 0.02$  ( $\equiv 50$  time steps) is sufficiently small to yield solutions independent of  $\Delta r^*$ .

The accuracy of the solution was examined using appropriate dimensionless material balance equation. The computed values of the concentration profiles were found to be in good agreement with the material balance equation.

## REFERENCES

1. W. K. Lu and G. Bitsianes: *Trans. TMS-AIME*, 1966, vol. 236, p. 531.
2. R. H. Spitzer, F. S. Manning, and W. O. Philbrook: *Trans. TMS-AIME*, 1966, vol. 236, p. 726.
3. J. H. Krasuk and J. M. Smith: *A.I.Ch.E.J.*, 1972, vol. 18, p. 506.
4. J. Szekely and J. W. Evans: *Met. Trans.*, 1971, vol. 2, p. 1699.
5. E. A. Mason, A. P. Malinauskas, and R. B. Evans: *J. Chem. Phys.*, 1967, vol. 46, p. 3199.
6. E. A. Mason and T. R. Marrero: *Adv. in Atom. and Mol. Phys.*, 1970, vol. 6, p. 155.
7. J. W. Evans: *Can. J. Chem. Eng.*, 1972, vol. 50, p. 811.
8. J. Douglas and T. M. Gallie, Jr.: *Duke. Math. Journal*, 1955, vol. 22, p. 557.
9. M. Lotkin: *Quart. App. Math.*, 1960, vol. 18, p. 79.
10. W. D. Murray and F. Landis: *Trans. ASME (J. of Heat Tr.)*, 1959, vol. 81, p. 106.